Facies analysis and diagenetic evolution of the Dinantian carbonates in the Dutch subsurface: data and analyses well S05-01

Report by SCAN

October 2019

Ministerie van Economische Zaken en Klimaat
ebn
TNO
Interreg North-West Europe DGE-ROLLOUT

Facies analysis and diagenetic evolution of the Dinantian carbonates in the Dutch subsurface: data and analyses well S05-01

Written by:
Mahtab Mozafari[1], Peter Gutteridge[2], Alberto Riva[3], Kees Geel[4], Joanna Garland[2] and Julie Dewit[2]

October 2019

1- Energie Beheer Nederland (EBN), Daalsesingel 1, 3511 SV Utrecht, the Netherlands
2- Cambridge Carbonates Ltd, No. 4 The Courtyard, 707 Warwick Road, Solihull, B91 3DA, UK
3- G.E.Plan Consulting srl, Via L. Ariosto 58, 44121 Ferrara, Italy
4- Geological Survey of the Netherlands (TNO), Princetonlaan 6, 3584 CB Utrecht, the Netherlands

Dit rapport is een product van het SCAN-programma en wordt mogelijk gemaakt door het Ministerie van Economische Zaken en Klimaat

Table of contents

13. S05-01

13.1 Introduction

The S05-01 well was drilled in 1981, in the offshore area of Zeeland (Figures 13-1 and 13-2, Table 13-1), close to the BHG-01 and S02-2 wells. It reached 2230 m TD in the Devonian Bollen Claystone. The well, drilled for hydrocarbon exploration, was dry. S05-1 was drilled offshore, spudded on 24/05/1981 and abandoned on 23/07/1981. The target of the well was the Lower Carboniferous Zeeland Formation.

Figure 13-1: Map showing all the wells penetrating the Dinantian carbonates. Location of the S05-01 well is indicated by a dashed red circle.

Table 13-1: Table summarising the coordinates of the S05-01 well (from www.nlog.nl).

Co-ordinates (x, y in utm31, ed50 format)	538850, 5738235
Lat/Long (°)	51.7925556, 3.5632778
Supplied co-ordinates	3.5632778, 51.7925556 (ED50-GEOGR)
Depth in meters referred to :	Rotary Table
Total depth (m, along hole) :	2230
Vertical position of Rotary Table :	28.65 meter relative to MSL
Trajectory shape :	Deviated
Deviation in X-direction :	35.89
Deviation in Y-direction :	13.43
True vertical depth (TVD) in m :	2228.764

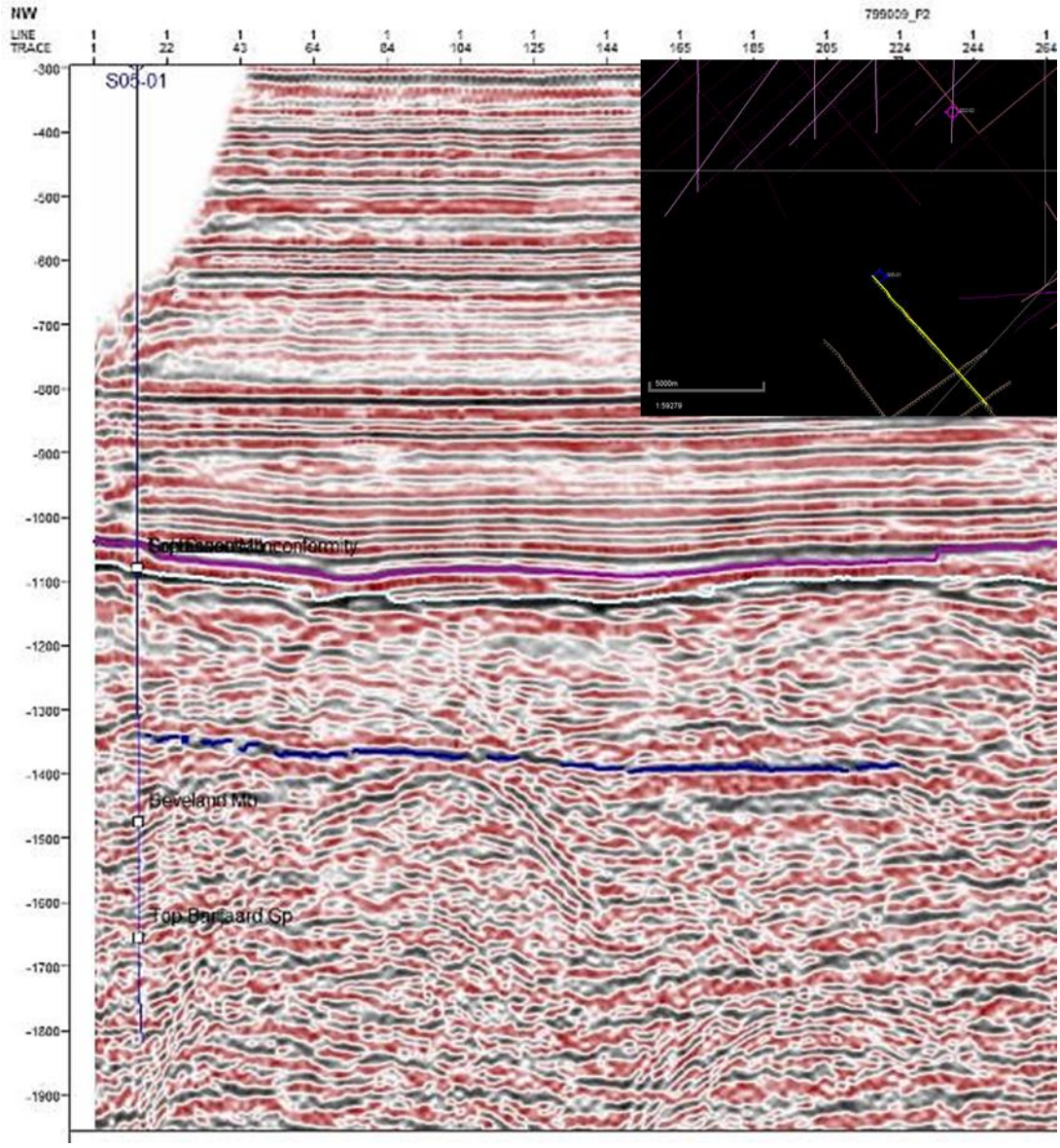

Figure 13-2: Seismic section with the location of well S05-01.

13.2 Available dataset

Most of the available data and reports on the S05-01well are available on "www.nlog.nl" within the following link:

https://www.nlog.nl/nlog/requestData/nlogp/allBor/metaData.jsp?type=ALLBOR&id=106526559

The most relevant publications discussing and presenting the data obtained from S05-01 well are as following:

Bless, M. J. M. (1982). Biostratigrafie van het Dinantien in de boring S 5-1 (NAM), trajeot 1190 - 2143.5 m. Heerlen.

Boulvain, F., and Poty, E. (2002). Analyse sedimentologique et stratigraphique du sondage S5-1.

Carlson, T. (2019). Petrophysical Report of the Dinantian Carbonates in the Dutch Subsurfaceacies analysis and diagenetic evolution of the Dinantian carbonates in the Dutch subsurface. SCAN Report, 26 p. Report downloadable from www.nlog.nl/scan

Muchez, P., Viaene, W. A., Keppens, E., Marshall, J. D., and Vandenberghe, N. (1991b). Vein cements and the geochemical evolution of subsurface fluids in the Campine Basin (Poderlee borehole, Belgium), Journal of the Geological Society of London, 148, 1005-1117.

NAM (1982). Critical Well Review, S 5-1. Assen.

Nielsen, P., Swennen, R., and Keppens, E. (1994). Multiple-step recrystallization within massive ancient dolomite units: an example from the Dinantian of Belgium. Sedimentology, 41, 567-584.

Pickard, N. A. H., and Gutteridge, P. (1997). Dinantian depositional systems and exploration potential: offshore and onshore, The Netherlands. Sedimentological study.

Racz, L. (1982). Subdivision and environment of deposition of the Lower Carboniferous carbonate sequence in well S 5-1, Nam. Assen.

Reijmer, J. J. G., Ten Veen, J. H., Jaarsma, B., and Boots, R. (2017). Seismic stratigraphy of Dinantian carbonates in the southern Netherlands and northern Belgium. Geologie En Mijnbouw/Netherlands Journal of Geosciences, 96(4), 353-379. https://doi.org/10.1017/njg.2017.33

TNO (2003). Toelichting bij kaartbladen Xl en Xll Middelburg-Breskens en Roosendaal-Terneuzen. Geologische Atlas van de Diepe Ondergrond van Nederland.

13.2.1 Logs

This well has a complete suite of logs (Figure 13-3) and has been petrophysically evaluated within the scope of the SCAN project (Carlson, 2019).

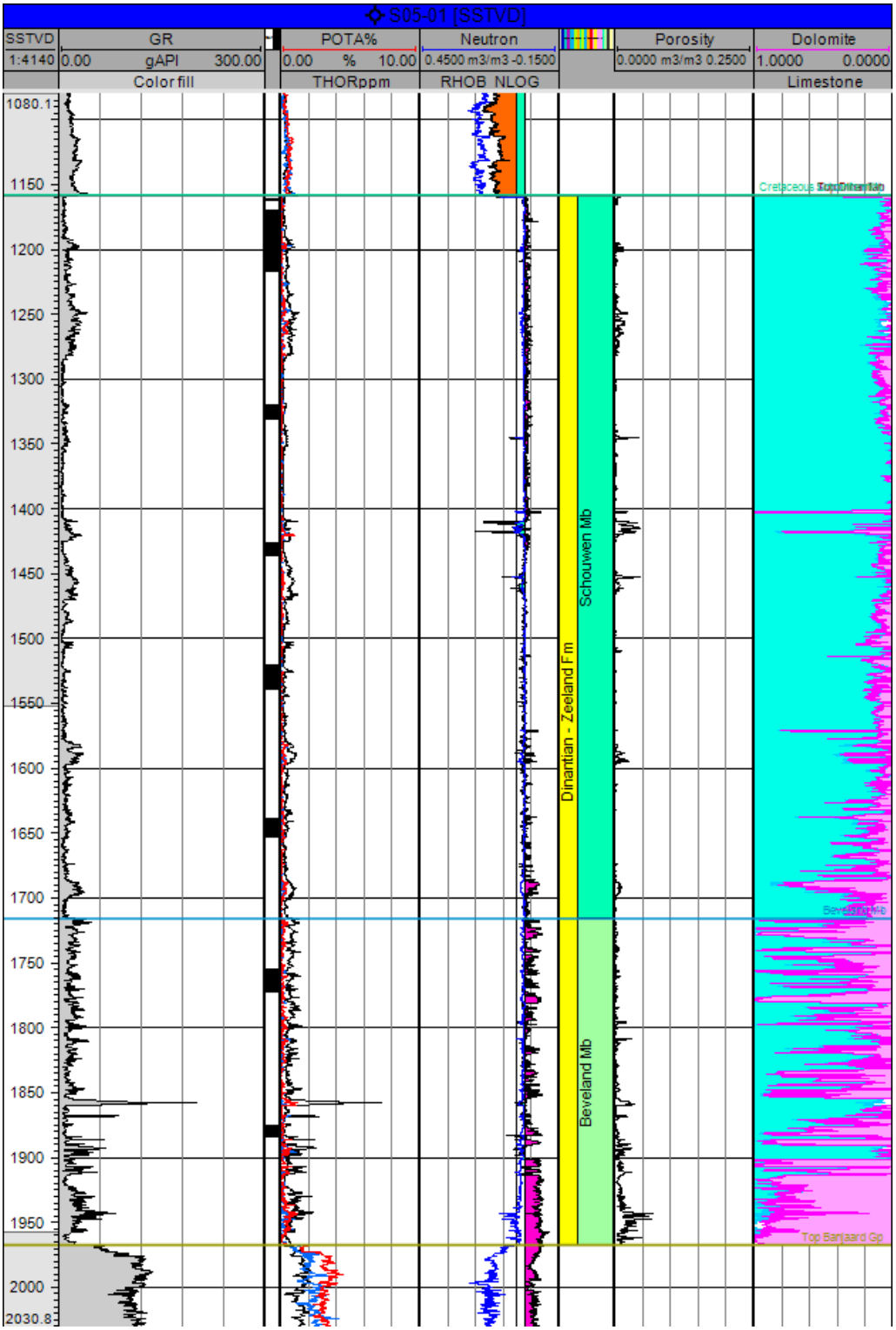

Figure 13-3: Gamma ray, neutron/density, porosity and mineralogical logs in the S05-01 well.

13.2.2 Cores, sidewall cores and cuttings

A total number of eleven cores are available for the S05-01 well. Short description of cores is given in Table 13-2. The graphical description (core logs) are presented in Appendix B as a supplementary document.

Table 13-2: Short description of the eleven cores available for S05-01 (from Pickard and Gutteridge, 1997).

S05-01	Top (m)	bottom (m)	total length	Formation	Member	Age	Depositional environment	Facies
Core 1	1190	1191.5	1.5		Schouwen	early Warnantian	Shallow high energy subtidal	Bioturbated bioclast peloid grain/packstone. Bioclastic packstones and grainstones containing abundant crinoid, shell debris.
Core 2	1199	1210	11		Schouwen	early Warnantian/Livian	Shallow high energy subtidal	Bioturbated bioclast peloid grain/packstone. Packstone and grainstone beds containing fine shell debris, crinoids and bioclastic peloids.
Core 3	1210	1228	18		Schouwen	Livian	Shallow high energy subtidal	Bioturbated bioclast peloid grain/packstone. Stacked beds of 'clean'grainstones containing large shells and fine crinoidal debris. Regular stylolitic surfaces.
Core 4	1228	1245.5	17.5		Schouwen	Livian	Shallow high energy subtidal	Bioturbated bioclast peloid grain/packstone. Oncoid-peloid grainstones with thick walled shell fragments. Locally chertified.
Core 5	1349	1360	11		Schouwen	Livian	Shallow subtidal	Bioclast peloid grain/packstone. Bioturbated wacke- to packstone containing thick shells (1-2 cm size), crinoid debris, rare bryozoan and coral fragments. Stylolites occur throughout the core.
Core 6	1455	1465	10		Schouwen	Upper Molinacian-lower Livian	Subtidal	Algal packstone/wackestone/bafflestone. Bioclastic graded beds: fining-up trend from cm-size peloids to 'micritic'carbonate mud. Levels of black siliciclastic shales interbedded. Horizontal stylolites and filled vertical fractures occur sporadically. The interval is strongly bioturbated.
Core 7	1550	1568	18		Schouwen	Molinacian	High energy subtidal	Fining-up grainstone cycles. Alternating beds consisting of bioclastic, bioturbated wacke- to grainstones. Occurrences of thick-walled shells of cm-size. Some beds slightly dolomitized, streaks of mouldic porosity.
Core 8	1668	1682	14		Schouwen	Lower Molinacian	fine bioclast peloid intraclast grain\packstone	Thickly bedded grain/packstone with shale beds
Core 9	1784	1802	18		Beveland	Earliest Molinacian	intraclast oncoid pack/grainstone cycles	shallow subtidal to peritidal cycles
Core 10	1904.5	1905.5	1		Beveland	no diagnostic fauna	High energy subtidal	dolomitised peloid grainstone
Core 11	1906	1913	7		Beveland	no diagnostic fauna	High energy subtidal	dolomitised peloid grainstone

13.2.3 Petrography and additional analyses

Several thin sections were prepared from well S05-01: Cores 1 to 4 (n=118), Core 5 (n=13), Core 6 (n=12), Core 7 (n=26), Core 8 (n=18), Core 9 (n=26), Cores 10 and 11 (n=14).
The new thin section descriptions (SCAN project) are integrated with those of Pickard and Gutteridge (1997). Moreover, a complete set of photomicrographs was prepared at NAM core store.
Additional samples were selected with the aim of understanding the origin of the dolomite (sample 1909.35 m) and the nature of calcite veins, i.e. irregular, possibly karst related, calcite veins (sample 1209.30 m) vs. hydrofractures (samples 1226.87 m and 1230.99 m). Four thin sections were made for cathodoluminescence petrography and 14 samples were drilled out at 12 core depths for stable isotope analysis (Table 13-3). Vitrinite reflectance measurements are available from TNO (2003) (Table 13-4).

Table 13-3: Overview of samples selected for additional analysis in the well S05-01.

Sample depth (m)	**CL**	**Stable isotopes**
1209.3	x	X (matrix and vein)
1222.62		x
1226.87	x	x
1230.94	x	X (matrix and vein)
1351.45		x
1457.7		x
1796.2		x
1801.7		x
1904.5		x
1905.8		x
1908.45		x
1909.35	x	xx

Table 13-4: Available vitrinite reflectance measurements for the well S05-01.

Depth (m MD)	%Rr
1275	1.20
1285	1.25
1885	1.68
1940	1.71
2035	1.24

13.3 Stratigraphy

The succession of the S05-01 well spans from Quaternary to the Devonian (Table 13-5), encountering the Cretaceous unconformity at 1187 m MD, over the Namurian and the Dinantian at 2230 m MD.

Table 13-5: Stratigraphy of the S05-01 well (from www.nlog.nl).

Stratigraphic unit	**Top interval**	**Base interval**
Upper North Sea Gp.	0	183
Rupel Clay Mb.	183	273
Vessem Mb.	273	317
Asse Mb.	317	447
Brussels Sand Mb.	447	510
Ieper Mb.	510	748
Basal Dongen Sand Mb.	748	780
Landen Clay Mb.	780	828
Ommelanden Fm.	828	1187
Schouwen Mb.	1187	1745
Beveland Mb.	1745	1996
Bosscheveld Fm.	1996	2005
Bollen claystone Fm.	2005	2230

13.3.1 Dinantian interval

The stratigraphic succession of the Dinantian carbonates is represented by the Schouwen and Beveland Members, for a total of 809 m. The succession entirely reflects a shallow water carbonate platform environment.

13.4 Biostratigraphy

The biostratigraphic attribution of the Zeeland Formation in the S05-01 well covers the intervals from Tournaisian until Lower Warnantian: the uppermost Warnantian is potentially missing due to the erosion linked to the Cretaceous unconformity (Table 13-6).

Table 13-6: Biostratigraphy of the S05-01 well.

	Top (m)	bottom (m)	Fauna	Foraminifera	Zone (Belgium)	
Cores 1 to 4	1190	1203.5		Asperodiscus	basis V3b	earliest Warnantian
Cores 1 to 4				Nodasperodiscus		
Cores 1 to 4				Archaediscus gr. Angulatus		
Cores 1 to 4	1203.5	1240.45			V2b-V3a	Livian
Core 4	1205	1359		Quasiendothyra nibelis	V2b-V3a	Livian
Core 4				Koskinotextularia		
Core 5	1349	1360			V2b-V3a	Livian
Core 6	1455	1465			V2a-V2b	Upper Molinacian-lower Livian
Core 6	1455	1462.8			V2a-V2b	
Core 7	1550	1568			V1a-V2a	Molinacian
Core 7 and 8	1556.3	1680			V1a-V2a	
Core 8	1668	1682	Koninckopora	NO archaediscids	Eoparastaffella Cf4 alpha	earliest Moliniacian
Core 9	1784	1802	Pachysphaerina pachysphaerica	NO archaediscids	Eoparastaffella Cf4 alpha	lowermost Moliniacian
Core 9	1784	1802	NO Koninckopora			
Core 9	1786.9	1799.8			basis V1a	
Core 10	1904.5	1905.5			Tournaisian	
Core 11	1906	1913			Tournaisian	
Core 11	1907	1908.2			?Tournaisian	
	2021.3				Tournasian / Fammenian	

13.5 Sequence stratigraphy

Nine depositional cycles were recognised in the S05-01 well (Figures 13-4 to 13-10); the last depositional cycle has been eroded, as the Dinantian succession is cut by the base Cretaceous unconformity.

Cycle 1a: This depositional cycle represents the initial flooding of the basin; the TST is thin and has a clean gamma ray character above the thick high gamma ray fine clastics at the top of the Tournaisian. This is interpreted as deposition of clean carbonates in shallow water which followed by increasing gamma ray related to deposition of more muddy carbonates in deeper water during the maximum flooding to early HST. The HST shows decreasing gamma ray and is interpreted as deposition on a shallower water carbonate ramp setting.

Cycle 1b: This depositional cycle contains a thin TST to maximum flooding interval, Cores 10 and 11 shows that HST to consist of thickly bedded, dolomitised bioclastic-peloid grainstone deposited in a high to moderate energy setting on the inner- to mid- part of a carbonate ramp (Figure 13-4).

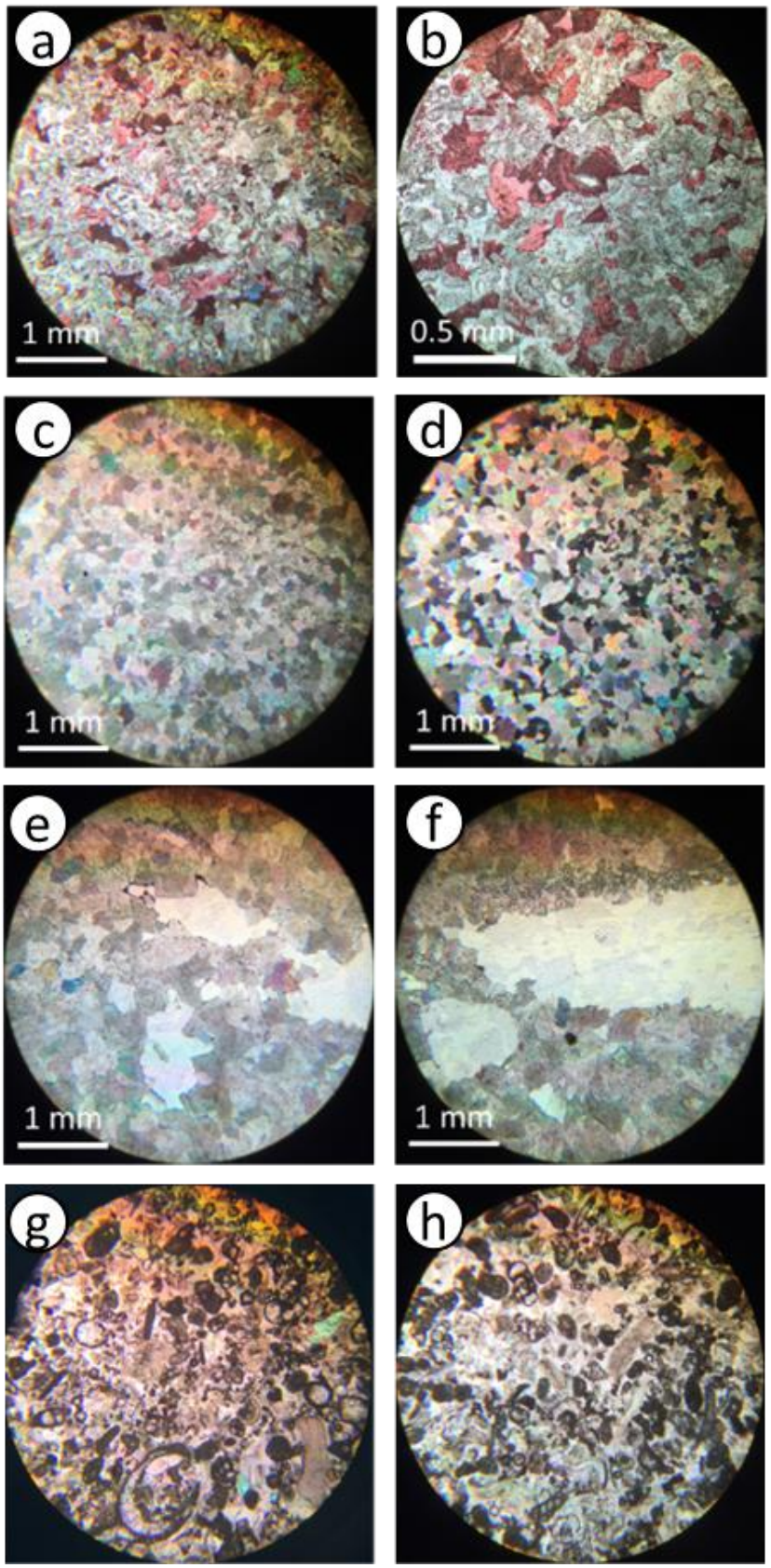

Figure 13-4: Microfacies represented in the 1b depositional cycle: a, b) Selective, partial dolomitisation (Core 10, 1907 m). c, d) Patchy, pervasive dolomitisation (Core 10, 1907 m). e, f) Dolomite with small mouldic pores (Core 11, 1910.50 m). g, h) Bioclastic-peloid grainstone (Core 11, 1911.20 m).

Cycle 1c: This depositional cycle comprises a relatively thick TST with a HST that has a moderately high gamma ray signature. Core 9 from the HST of the 1c depositional cycle consists of cyclic shallow subtidal to peritidal shallow ramp carbonates with cycle tops marked by peritidal facies. The subtidal facies are dominated by oncoids, other coated and highly micritised grains suggesting deposition took place in a relatively restricted shallow carbonate ramp setting. Microfacies includes algal boundstone-coated grain and bioclastic grainstone, bioclastic-peloid grainstone (some with ostracods) and dolomite (Figure 13-5).

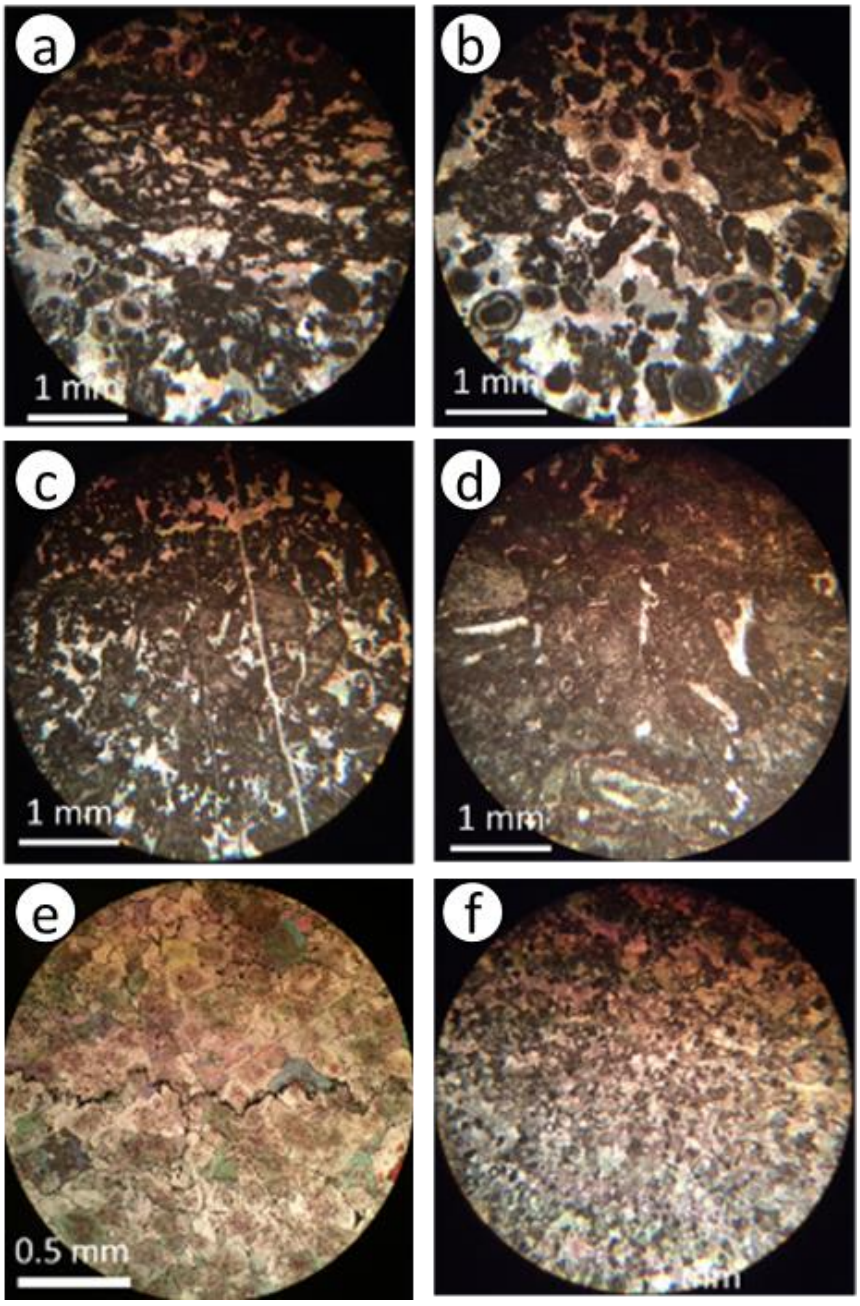

Figure 13-5: Microfacies represented in the 1c depositional cycle: a, b) Algal boundstone-coated grain grainstone (Core 9, 1786.90 m). c, d) Coated grain-bioclastic grainstone (Core 9, 1789 m and 1790.80m).e) Dolomite pre-dating stylolite (Core 9, 1789.90 m). f) Bioclastic-peloid grainstone (Core 9, 1795.30 m).

Cycle 1d: This depositional cycle consists of a relatively thin low gamma ray TST passing up into a high gamma ray interval interpreted as a maximum flooding interval. Core 8 is representative of this depositional cycle and consists of thickly bedded bioclastic grainstone/packstone with intraclasts, bioclasts and coated grains deposited in an inner to mid ramp depositional setting; microfacies includes fine bioclastic (- peloid) pack-grainstone and bioclastic - coated grain grainstone (Figure 13-6).

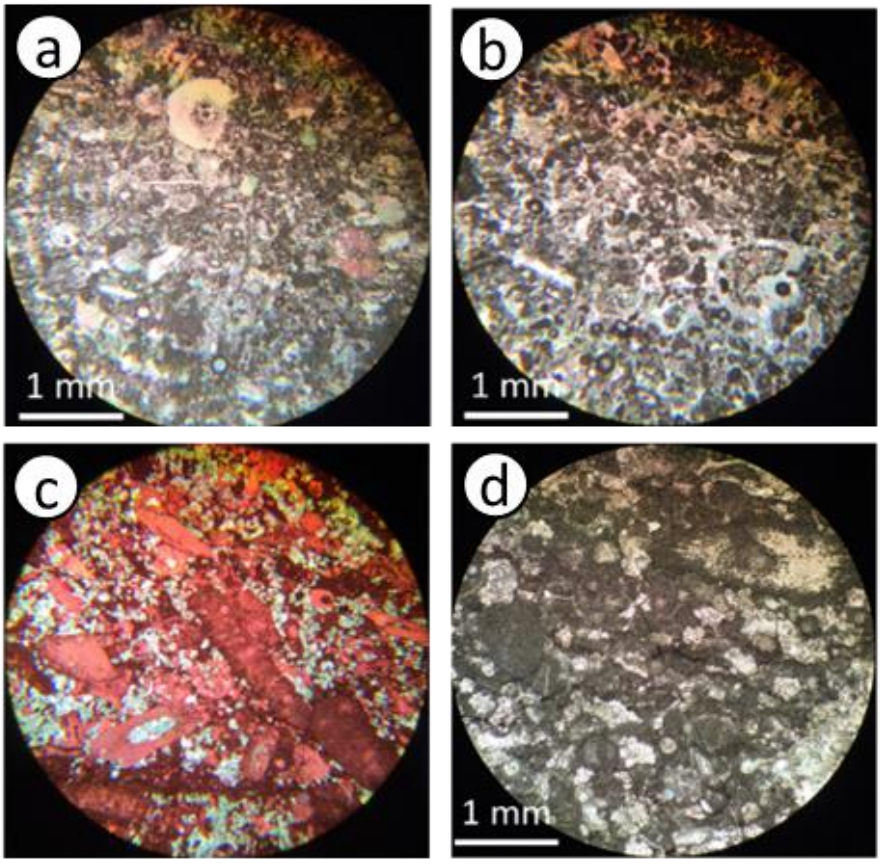

Figure 13-6: Microfacies represented in the 1d depositional cycle: a, b) Fine bioclastic (-peloid) pack-grainstone (Core 8, 1670.70 m and 1673.40 m). c) Partially dolomitised pack-grainstone (Core 8, 1676.20 m). d) Bioclastic-coated grain grainstone (Core 8, 1681.20 m).

Cycle 2a: This depositional cycle consists of moderate gamma ray TST passing up into a high gamma ray interval interpreted as a deeper maximum flooding interval. Core 7 represents the low gamma ray HST and consists of medium- to thickly-bedded bioclastic packstone/grainstone with some coated grains deposited in an inner carbonate ramp setting; microfacies includes fine bioclastic grainstone and bioclastic-coated grain-peloid grainstone (Figure 13-7).

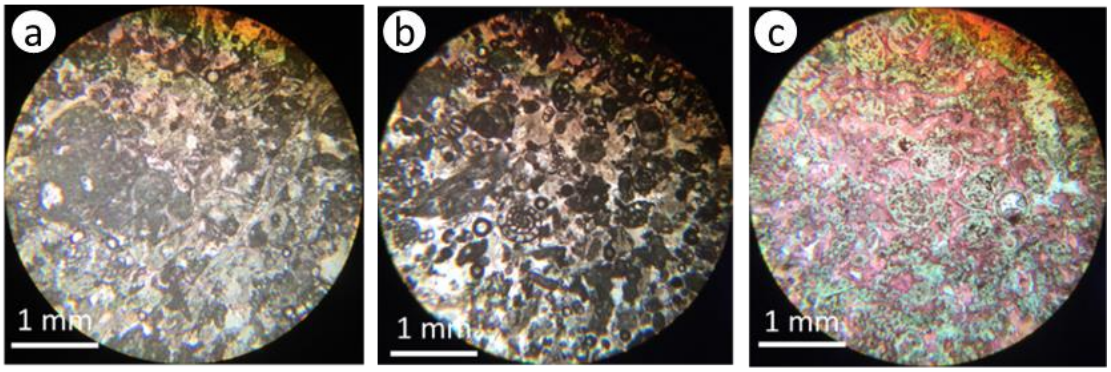

Figure 13-7: Microfacies represented in the 2a depositional cycle: a) Bioclastic-coated grain-peloid grainstone (Core 7, 1564.50 m). b) Fine bioclastic grainstone, sometimes partially silicified-peloid grainstone (Core 7, 1560.80 m and 1564.15 m).

Cycle 2b: This depositional cycle consists of a thin TST with increasing-upward gamma ray towards a high gamma ray maximum flooding interval with an overlying decreasing-upwards gamma ray HST. Cores 6 and 5 were taken in the early and late HST respectively which in the uppermost part of the HST it consists of medium-bedded bioclastic grainstone/packstone with some coated and micritised grains. This was deposited in a high energy setting above normal wave base, in an inner carbonate ramp or carbonate shelf interior. Microfacies includes bioclastic peloid grainstone with abundant large foraminifera and bioclastic-coated grain-peloid grainstone (Figure 13-8).

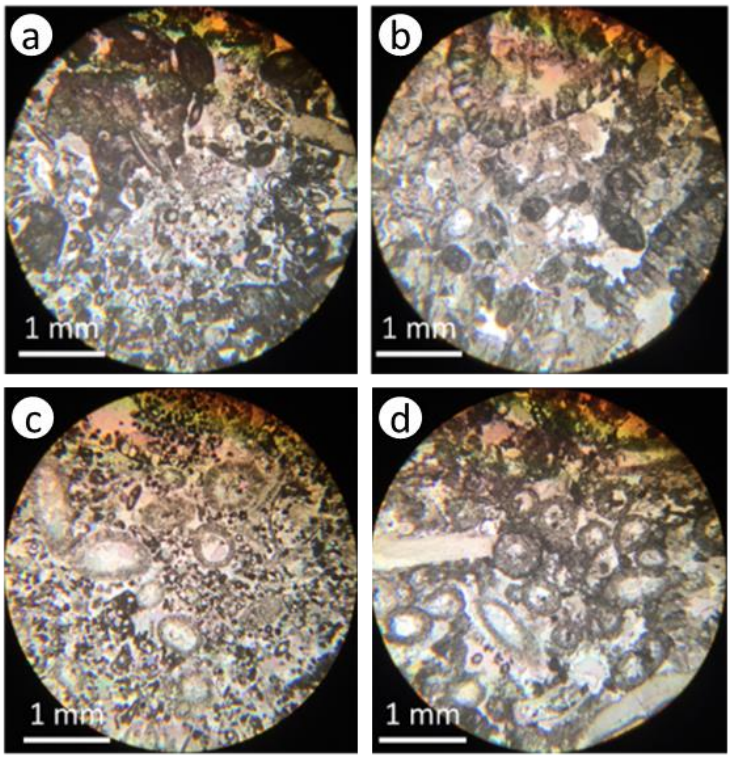

Figure 13-8: Microfacies represented in the 2b depositional cycle: a, b) Bioclastic-coated grain-peloid grainstone (Core 5, 1358.10 m and Core 6, 1456.50 m). c, d) Bioclastic-peloid grainstone (Core 5, 1350 m and Core 6, 1463.70 m).

Cycle 2c to 3a: These depositional cycle have a thin TST with increasing gamma ray towards a high gamma ray maximum flooding interval with a lower gamma ray HST. Cores 1 to 4 represent the HST where it consists of medium-bedded bioclastic grainstone/packstone with some coated and micritised grains. There is no indication of emergence within the cores. This suggests these depositional cycle were deposited in a moderate to high energy setting above or near normal wave base on a carbonate shelf interior. Microfacies includes bioclastic-coated grain-peloid grainstone, crinoidal pack-grainstone, fine bioclastic pack-grainstone and bioclastic- peloid grainstone (Figure 13-9).

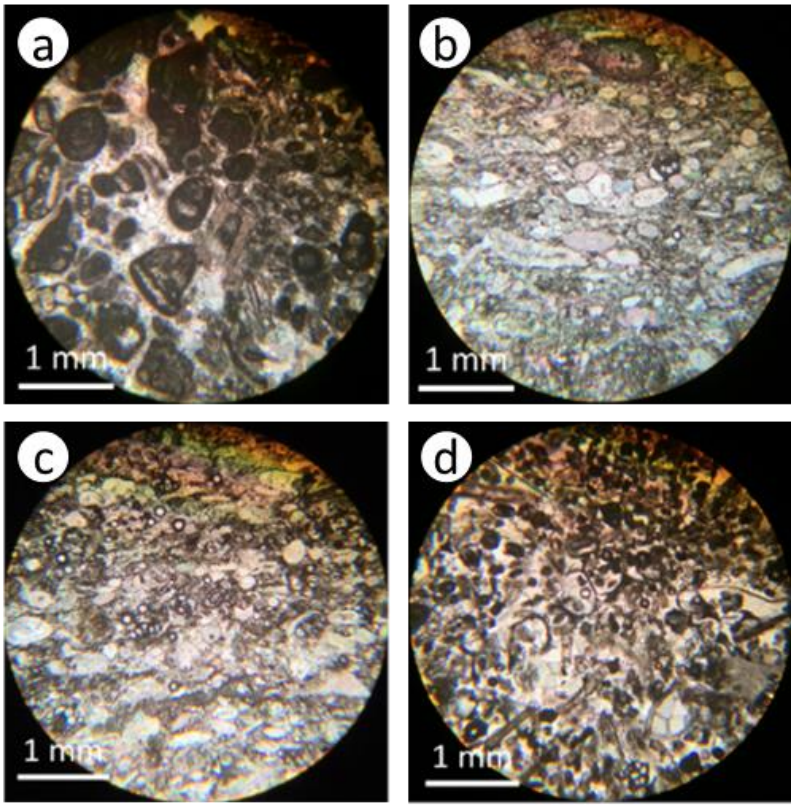

Figure 13-9: Microfacies represented in the 2c to 3a depositional cycle: a) Bioclastic-coated grain-peloid grainstone (Core 1, 1190 m). b) Crinoidal pack-grainstone (Core 3, 1221.80 m). c) Fine bioclastic pack-grainstone (Core 3, 1224.20m). d) Bioclastic-peloid grainstone (Core 2, 1209.80 m).

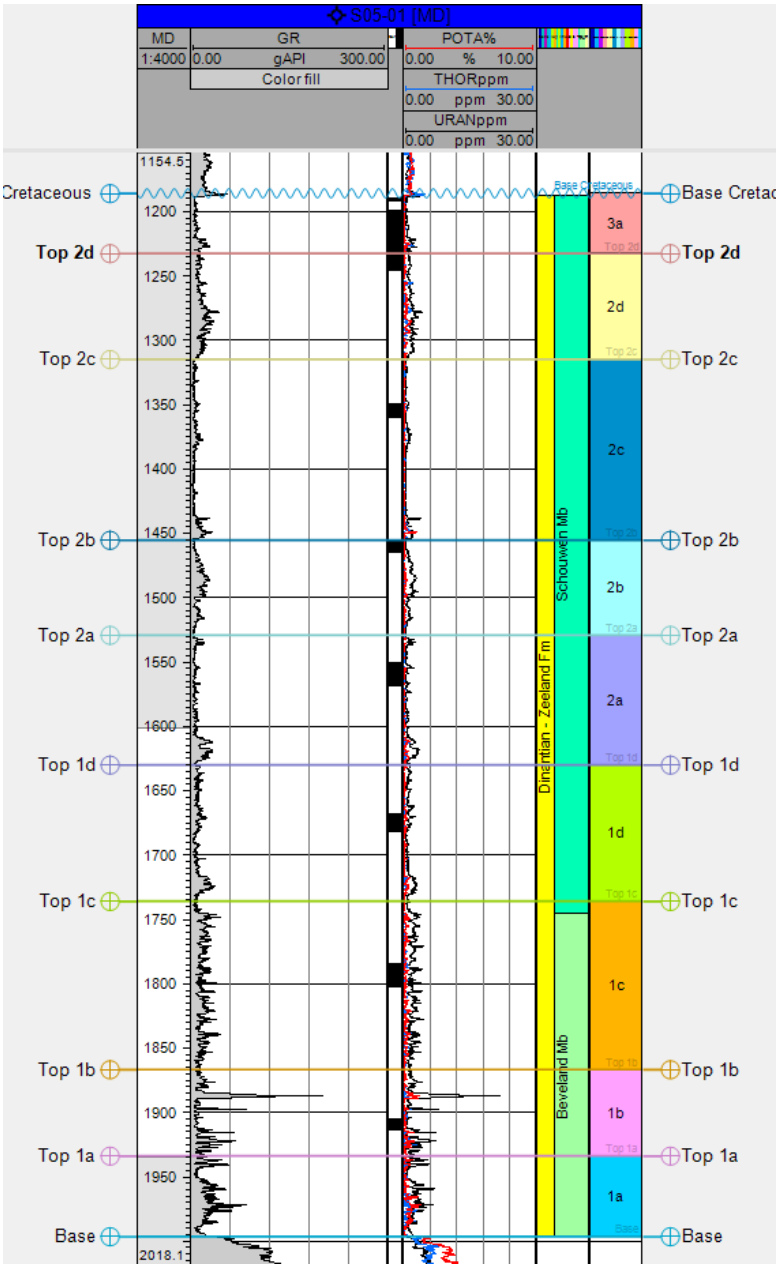

Figure 13-10: Depositional cycles recognised in the well S05-01.

The Dinantian carbonates in this well are overlain by the sub-Cretaceous unconformity. The Dinantian contains various karst features including fractures that have been enlarged by dissolution. Some Dinantian bioclasts are present in some karst cavities suggesting that these are either intra-Dinantian or near end-Dinantian. It is difficult to conclusively prove in which phase other karst features were formed owing to lack of infill. However, some that post-date burial diagenetic features such as stylolites suggest that these were associated with the sub-Cretaceous karst.

13.6 Diagenesis

13.6.1 Paragenetic sequence

A paragenetic sequence has been inferred from the thin sections analysis (Figures 13-11 to 13-15).

C1: Fibrous-columnar calcite cement lining bioclasts and pores. Generally isopachous and circumgranular. C1 and C2 are not observed together and may be mutually exclusive either marine or meteoric cementation occurs.

C2: Dogtooth-columnar calcite cement. The cement fringes bioclasts, but does not have a constant thickness. In general this cement occurs around fragments or individual bioclats in "floating" in C3 cement.

C3: coarse crystalline blocky calcite with crystal twins. This calcite phase occludes pores.

Veins cemented by calcite (C3?) cross cut by stylolites. Occasionally the cement is slightly ferroan. Stylolites contain pyrite and some are opened as calcite vein and are preferential sites for precipitation of Quartz. The studied sample also contain extensional and crack seal veins but their relative timing with stylolites are unknown. The calcite post-dating dolomitisation is C3 or different phase, i.e. C4? The calcite generation precipitating in stylolites is C4.

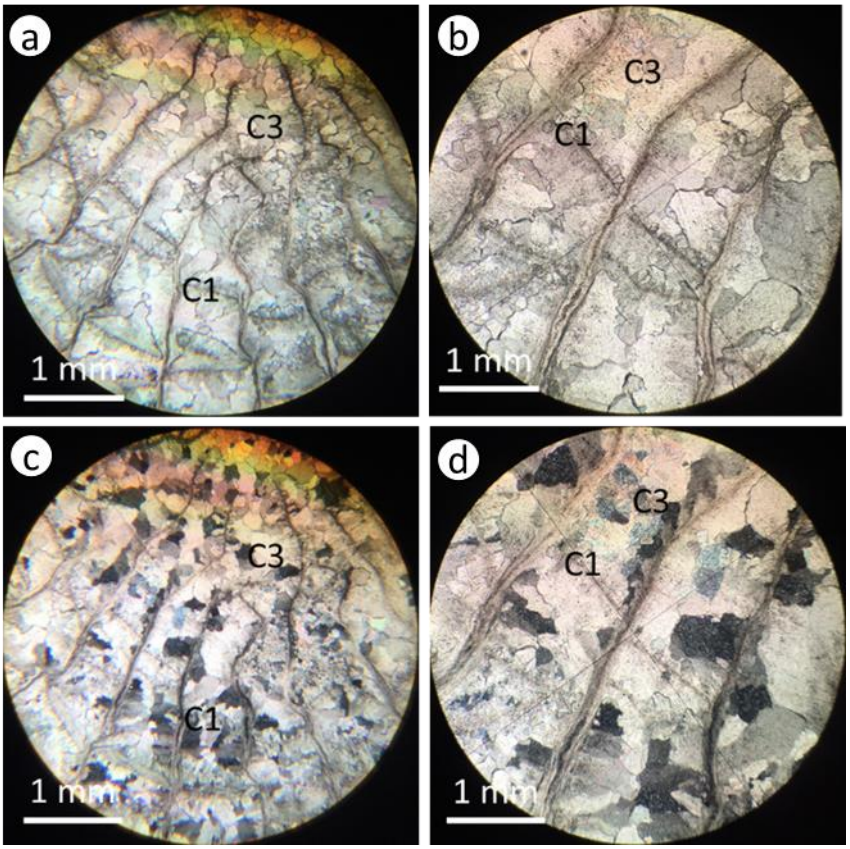

Figure 13-11: Fibrous calcite cement (C1) and pore occluding blocky calcite partially assimilating C1 (C3) 1557.65 m.

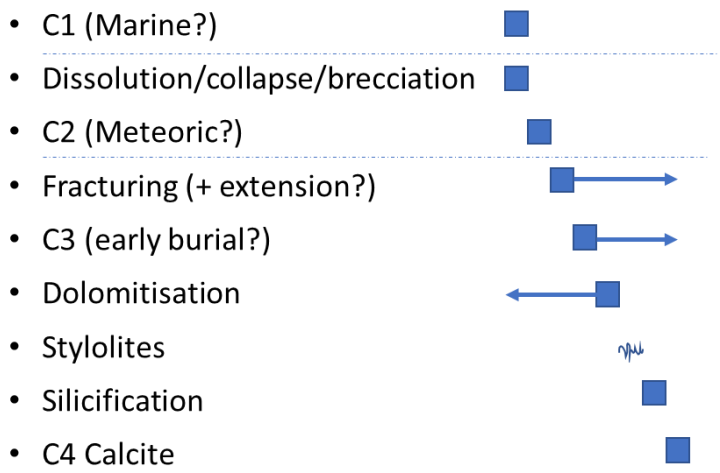

Figure 13-12: Inferred paragenetic evolution for the S05-01 well.

Evidence of karst and dolomitisation: minor collapse and brecciation of the host rock, generally limited to (dissolution enhanced) veins. No secondary porosity is related to the dissolution is preserved. Pores are occluded by C3 calcite cement. Dolomitisation is associated with minor secondary pores. These pores are often cemented by a later calcite cement (Figure 13-15).

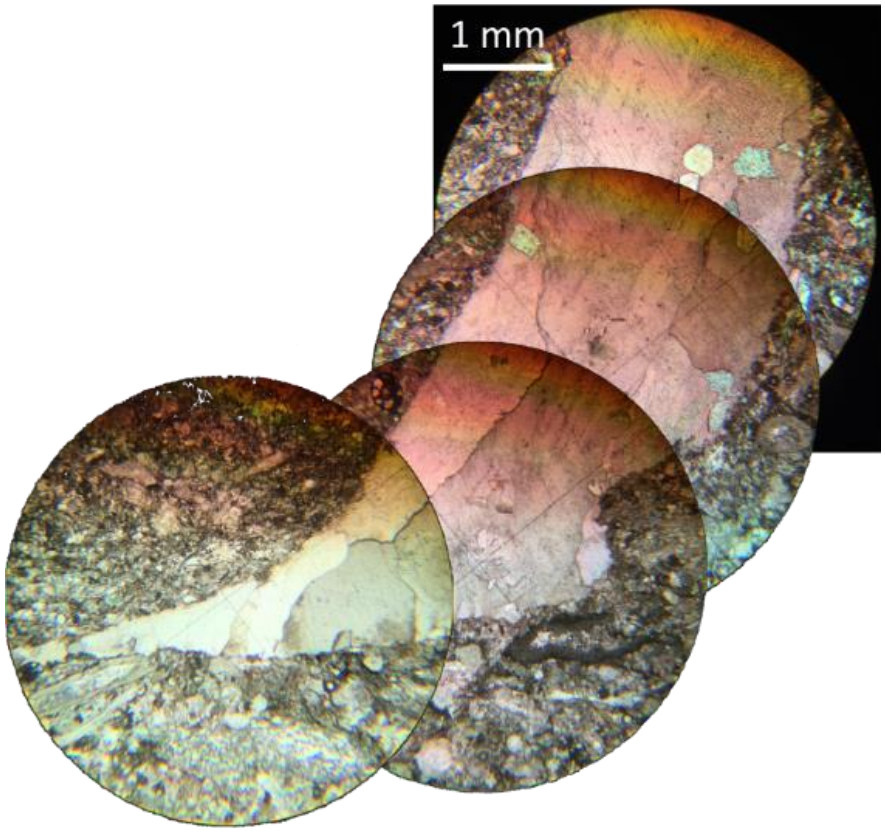

Figure 13-13: Dissolution enhanced fracture with rounded margins and variable width possibly of karstic origin (1223.40 m).

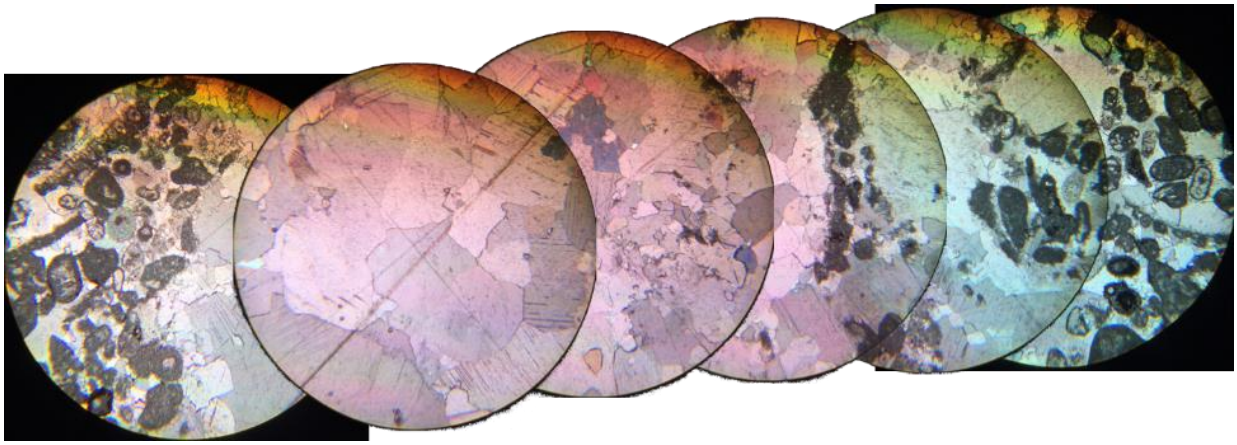

Figure 13-14: Fragments with dogtooth calcite cement (C2) and vein cemented by coarser calcite (C3) 1353.60 m.

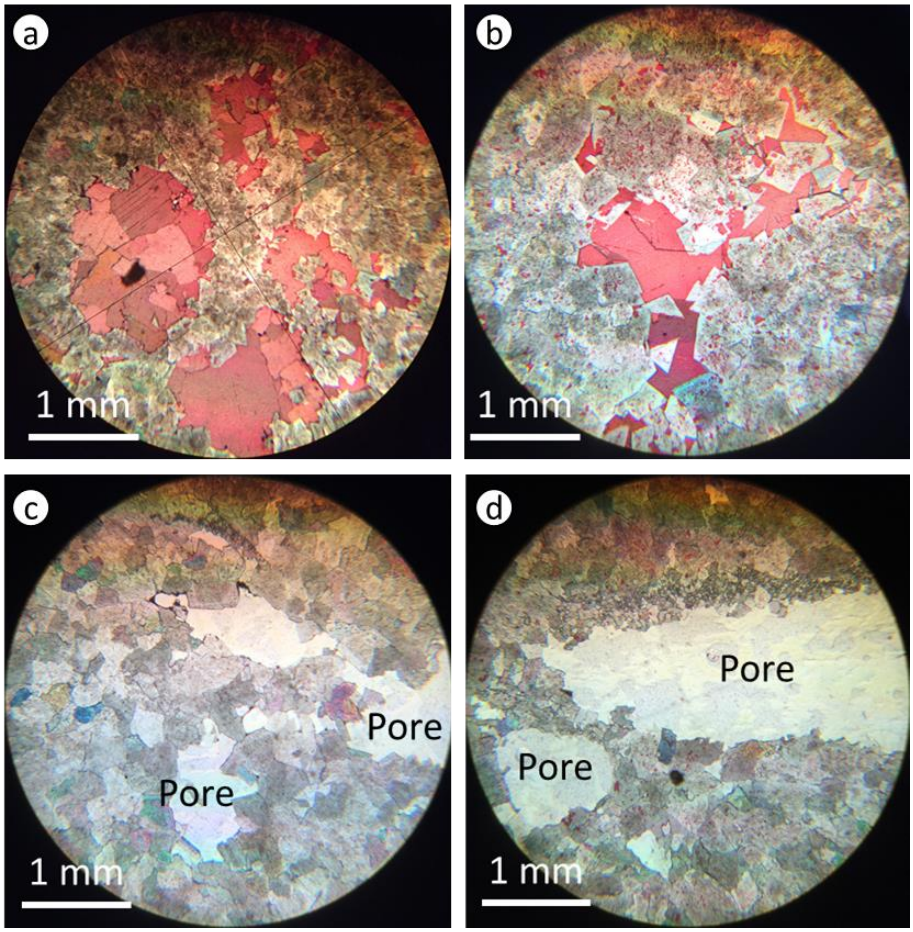

Figure 13-15: a, b) Dolomite with mouldic pores occluded by a later calcite cement (1796.20 m). c, d) Dolomite with small mouldic pores (1910.50 m).

13.6.2 Cathodoluminescence

Matrix dolomite/1909.35 m: The dolomite is generally dull red luminescent. Saddle dolomite crystals display a brighter luminescent rim (Figure 13-16a to d). Locally, a non- and bright luminescent calcite post-dates the dolomite (Figure 13-16e and f).

Irregular calcite vein/1209.30 m: The limestone host rock of sample 1209.30 m is cemented by finely zoned bright and dull luminescent calcite and non-luminescent calcite (Figure 13-17a and b). The veins cross cutting the host rock has an irregular outline and is cemented by blocky calcite with a dull to bright luminescence. The luminescence patterns is generally speckled with bright spots which may result of the many impurities in the calcite. Where the calcite is more limpid a more homogenous luminescence can be observed (Figure 13-17c to e). Could also be interpreted as neomorphic recrystallisation.

Hydrofracture calcite vein/1226.87 m and 1230.99 m: Hydrofractures with sigmoidal step-overs are cemented by elongated calcite crystals indicating opening/extension of the fractures took place during precipitation. The calcite is generally dull luminescent. Along crystal boundaries and a later bright luminescent calcite can be observed (Figure 13-19).

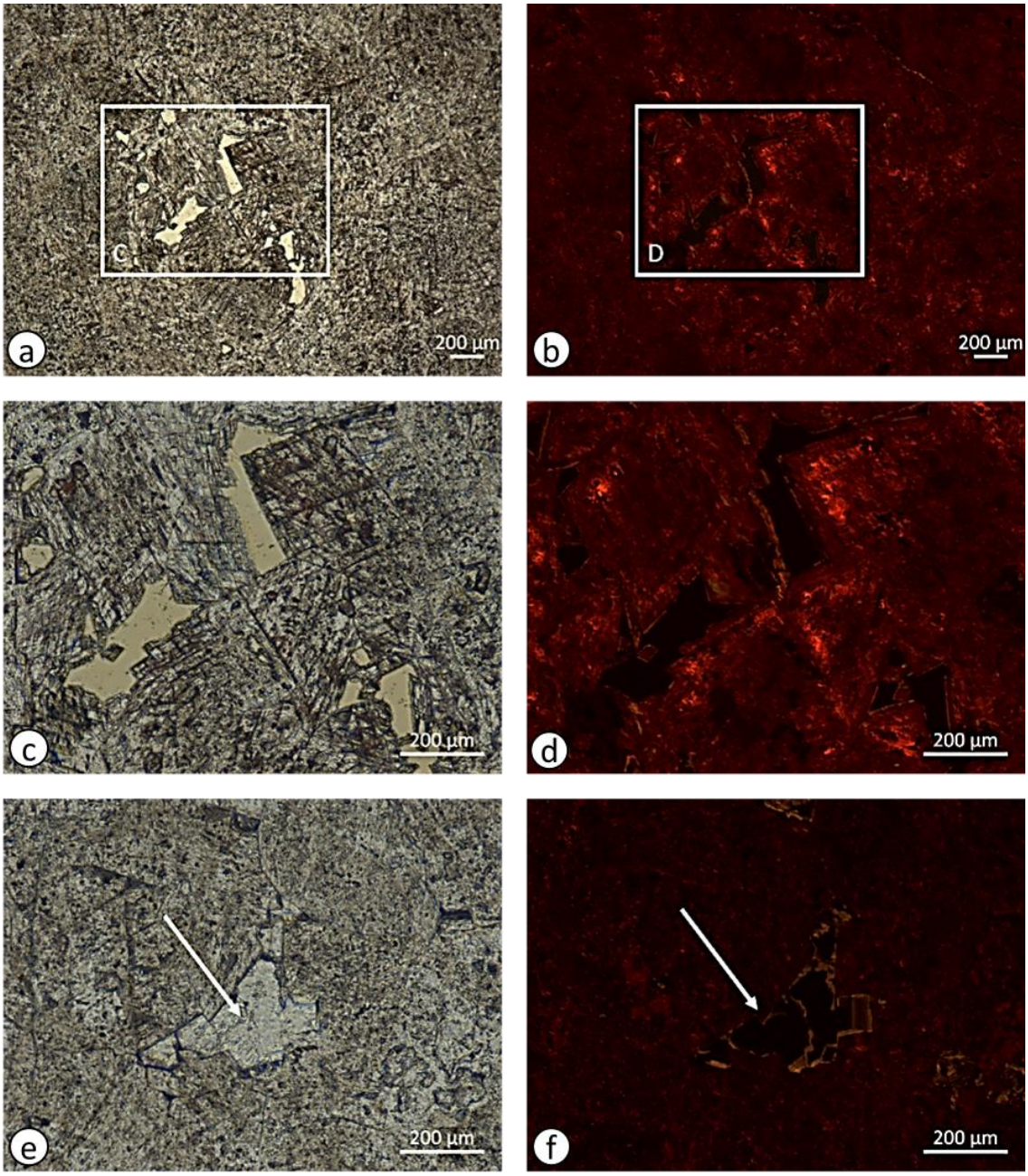

Figure 13-16: Equivalent PPL (plane polarised light) and CL microphotographs (cathodoluminescence): a-d) The matrix dolomite is generally dull luminescent with occasional bright luminescent zones (1909.35 m). e, d f) A non- and bright luminescent calcite (white arrow) locally occludes intercrystalline pores.

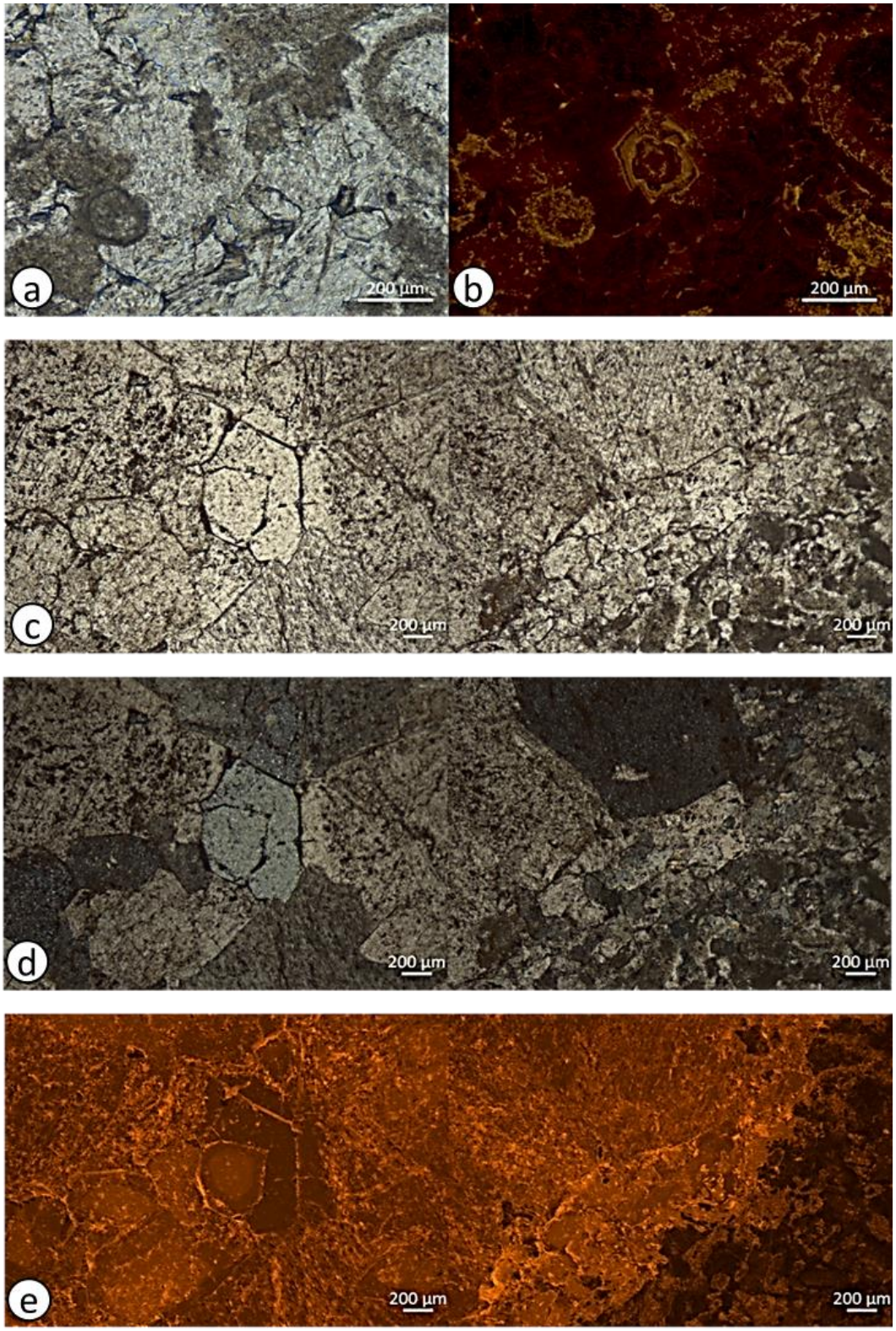

Figure 13-17: a, b) Equivalent PPL and CL microphotographs. The components of the limestone host rock are cemented by a finely zoned, bright and dull luminescent calcite followed by a non-dull luminescent calcite (1209.30 m). d, e) Equivalent PPL (plane polarised light), XPL (cross polarised light) and CL (cathodoluminescence) microphotographs. The calcite cementing veins with an irregular outline has a bright and dull luminescence. The speckled bright luminescence results of small impurities in the calcite. Where the calcite is more limpid the luminescence pattern is more homogenous and dull (1209.30 m).

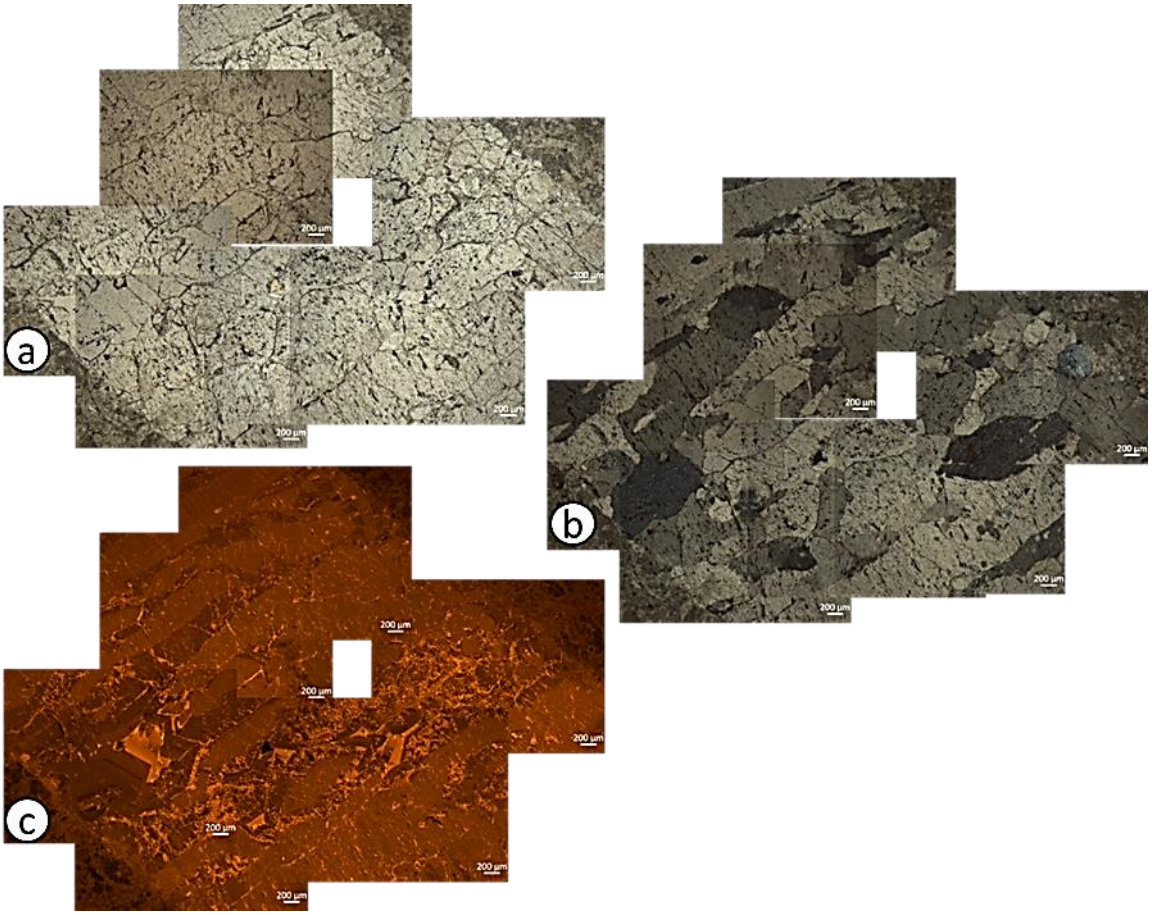

Figure 13-18: Equivalent PPL (a), XPL (b) and CL (c) microphotographs. Calcite cementing the extensional veins is characterised by a dull luminescence. A later phase of bright luminescent calcite resulted in recrystallisation along crystal boundaries (1230.99 m).

13.6.3 Stable isotopes

The stable isotope signature of the limestone host rock of the S05-01 samples is characterised by depleted $\delta^{18}O$ values similar to that of the other wells (Figure 13-19). The matrix dolomite samples fall within the same range. The calcite veins have slightly more depleted $\delta^{18}O$ values compared to the host rock. The calcite in the irregular and extensional veins have rather similar isotope signatures. They may nevertheless have different origins as diagenetic products of both warm and meteoric fluids can be characterised by depleted $\delta^{18}O$ values. The $\delta^{13}C$ values of all samples fall within the marine range (Table 13-7).

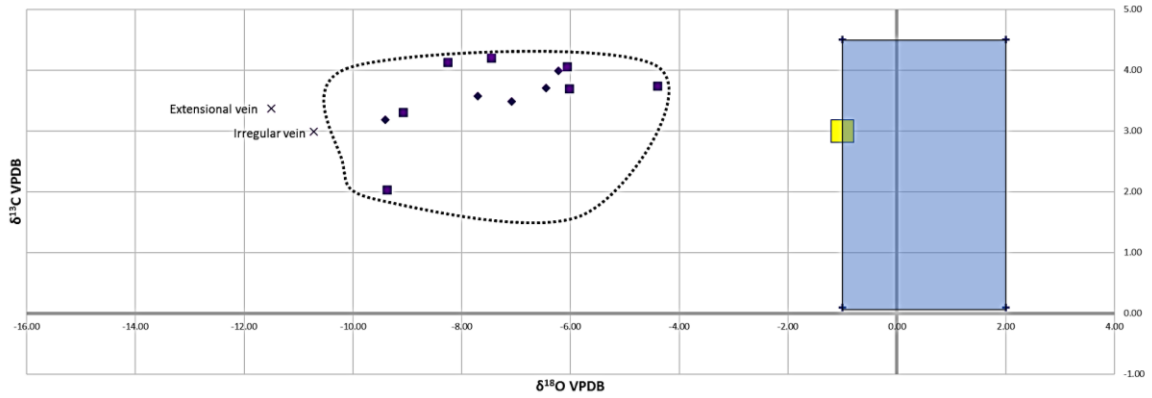

Figure 13-19: Stable isotope cross plot of the S05-01 samples. The calcite matrix, dolomite matrix and calcite veins are represented by squares, diamonds and cross symbols, respectively. The dotted line represents the limestone host rock/matrix signature obtained from the other studied wells with the exception of UHM-02. The Dinantian marine carbonates reference values are represented by yellow and blue area (after Muchez et al., 1991; Nielsen et al., 1994).

Table 13-7: Stable isotope results of the S05-01 samples expressed in per mill VPDB.

Sample depth (m)	Mineralogy	Matrix/vein	$\delta^{13}C$	$\delta^{18}O$
1209.3	Calcite	Vein	2.99	-10.7
1209.3	Calcite	Matrix	2.03	-9.37
1222.62	Calcite	Matrix	4.2	-7.46
1226.87	Calcite	Matrix	4.13	-8.26
1230.94	Calcite	Vein	3.37	-11.5
1230.94	Calcite	Matrix	4.06	-6.07
1351.45	Calcite	Matrix	3.7	-6.03
1457.7	Calcite	Matrix	3.31	-9.08
1796.2	Dolomite	Matrix	3.99	-6.22
1801.7	Calcite	Matrix	3.74	-4.41
1904.5	Dolomite	Matrix	3.19	-9.41
1905.8	Dolomite	Matrix	3.71	-6.45
1908.45	Dolomite	Matrix	3.49	-7.08
1909.35	Dolomite	Matrix	3.57	-7.71

13.6.4 Burial/thermal history

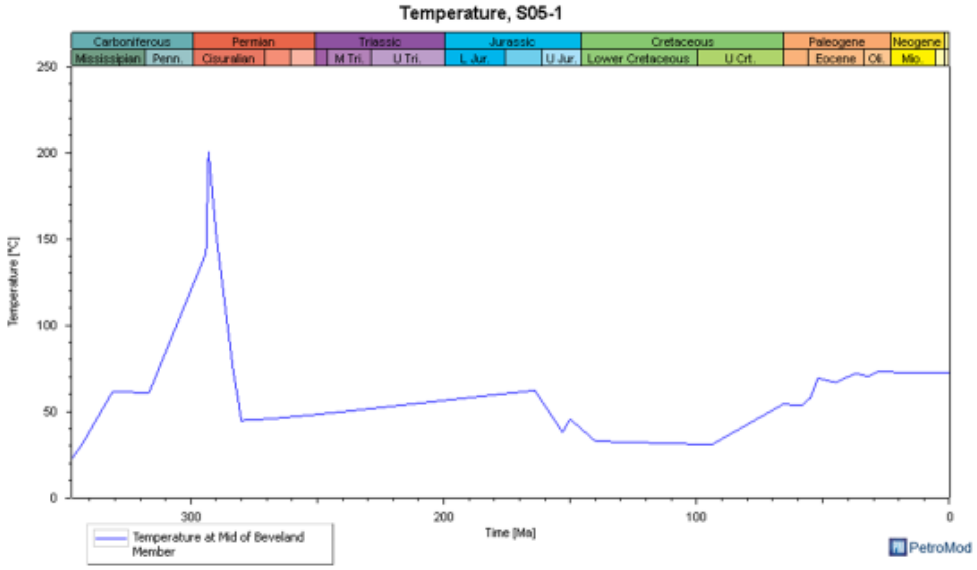

Figure 13-20: Computed temperature evolution for the Beveland Member in well S05-01.

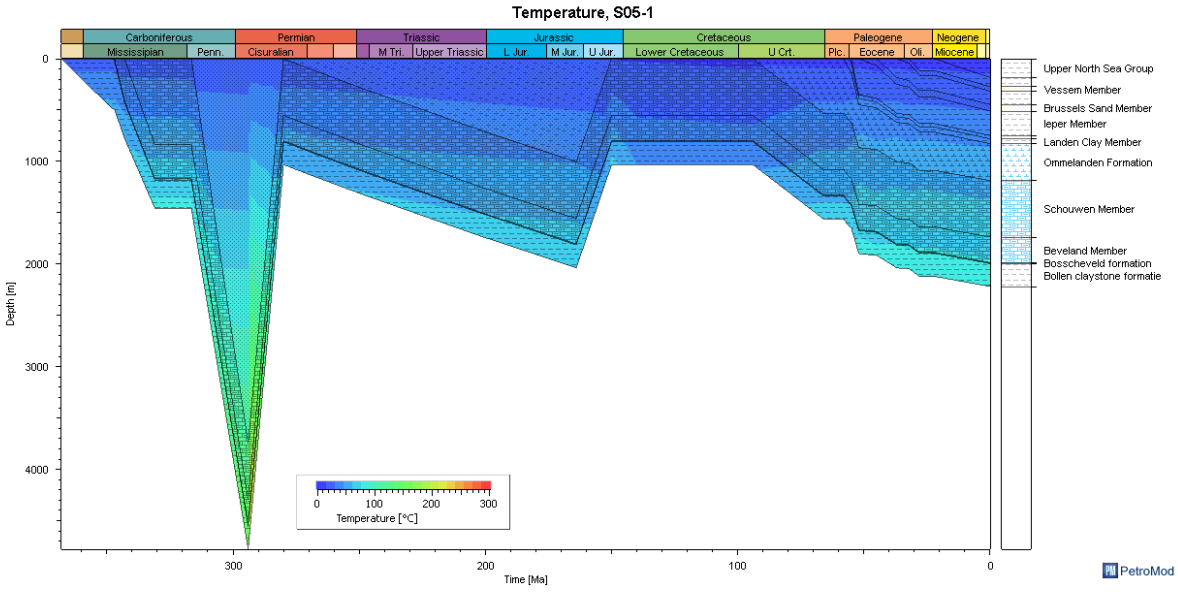

Figure 13-21: Burial history and temperature evolution computed for S05-01 well.

This page intentionally left blank

Daalsesingel 1
3511 SV Utrecht
scan@ebn.nl
www.scanaardwarmte.nl

Onderzoek in de ondergrond voor aardwarmte